

# The MROI's capabilities for imaging geosynchronous satellites

John Young<sup>a</sup>, Christopher Haniff<sup>a</sup>, David Buscher<sup>a</sup>,  
Michelle Creech-Eakman<sup>b</sup>, Ifan Payne<sup>b</sup>, Colby Jurgenson<sup>b</sup>, Van Romero<sup>b</sup>

<sup>a</sup> Cavendish Laboratory, University of Cambridge, JJ Thomson Avenue, Cambridge CB3 0HE, UK;

<sup>b</sup>Magdalena Ridge Observatory, New Mexico Institute of Mining and Technology, Socorro, NM,  
87801

## ABSTRACT

Interferometry provides the only practicable way to image meter-scale structure in geosynchronous satellites. This capability represents a unique commercial opportunity for astronomical interferometry, but to date no interferometer has been able to make an image of such a satellite. We discuss the challenges of imaging these objects and present results of sensitivity calculations and imaging simulations which show that the Magdalena Ridge Observatory Interferometer is likely to be well-suited to this application. Our preliminary results suggest that a significant proportion of GEO targets may be accessible and that it may be possible to routinely extract key satellite diagnostics with an imaging capability that would be able to distinguish, for example, 70 cm features on a 5-meter satellite bus and payload, 30 cm features on a 2-meter satellite bus or similarly sized structure, as well as precise quantitative information on much larger structures such as 10 m long solar panels. Optimised observation and data reduction strategies are likely to allow these limits to be improved in due course.

**Keywords:** interferometry, imaging, geosynchronous satellite

## 1. INTRODUCTION

The Magdalena Ridge Observatory Interferometer (MROI) project is an international collaboration between the New Mexico Institute of Mining and Technology (NMT) and the Astrophysics Group of the Cavendish Laboratory at the University of Cambridge in the UK to build the world's most ambitious and sensitive optical/near-infrared imaging interferometer. The MROI offices are located on the campus of New Mexico Tech in Socorro, New Mexico, and the observatory site is located on a ridge just south of South Baldy in the Magdalena Mountains, about 48 km (30 miles) west of Socorro, at an elevation of approximately 3,120 meters (10,460 ft) above sea level.

The MROI has been designed to be the world's leading, high-sensitivity optical/near-infrared facility interferometer. It will comprise an array of up to ten 1.4-meter diameter unit telescopes (UT) arranged in an equilateral "Y" configuration. Each of these UTs will collect light from a celestial source and send a collimated, stabilized beam of light to a laboratory facility located close to the array. There, the beams will be path-equalized and superposed to generate interference fringes that encode information about the brightness distribution of the source. In this way, diffraction-limited imaging with an effective angular resolution given by the largest inter-UT separation will be realized.

The MROI's unit telescopes will be re-locatable amongst a set of 28 separate foundation pads, so as to give inter-telescope separations (i.e. baseline lengths) from 7.8 meters to 346 meters. At its shortest operating wavelength, the MROI will have a maximum angular resolution of approximately 0.35 milliarcseconds. It will thus be able to resolve targets one hundred times smaller than those resolvable with the Hubble Space Telescope (HST), or indeed by all ground-based optical telescopes that might be deployed in the next few tens of years.

From the outset, the MROI has been designed to satisfy multiple user communities. One of its core missions will be to provide a tool for the commercial, military and intelligence communities to support space situational awareness. This paper provides an exploration of the MROI's capabilities in this role which were first discussed in Bakker et al 2009<sup>1</sup>. In the following sections we provide an introduction to the MROI, we discuss how well matched its sensitivity and speed of

operation are to the observation of typical GEO targets, and we provide a preliminary assessment of the diagnostic utility of interferometric imaging of such targets with an array like the MROI.

## 2. CURRENT STATUS OF GEO IMAGING

Imaging of most GEO targets is difficult with ground-based telescopes. At near-infrared wavelengths, even a 10m-class telescope with full adaptive optics correction is limited by diffraction to resolving scales of 8 meters or more at the distance of geosynchronous orbit. This is clearly inadequate for distinguishing features on satellite buses with typical dimensions of 3–8 m. To achieve sub-meter scale imaging would require a diffraction-limited telescope at least 50 meters in diameter, but even the next generation of giant astronomical telescopes, with billion-dollar price tags, will be only 30 meters or so in diameter. Thus it is unrealistic to expect this kind of capability from a ground-based filled-aperture telescope in the near or medium term.

An alternative to large monolithic telescopes comes from interferometry with arrays of more modest-sized telescopes. Astronomical interferometers such as CHARA and VLTI are now producing images with angular resolutions far exceeding those of a 50-meter telescope. Thus in principle interferometry delivers the angular resolution required to tackle the GEO imaging problem. However, there are two key problems that have hampered the use of interferometry in this domain. The first is that most current interferometers are only suited to imaging relatively bright objects, brighter than the majority of GEO targets unless these are “glinting”<sup>2</sup>. The second is that most existing interferometer arrays do not have enough telescopes to make images of complex geostationary objects. The design of the MROI interferometer overcomes these limitations.

## 3. KEY MROI DESIGN FEATURES RELEVANT TO GEO IMAGING

The primary functional goal of the MROI is to deliver model-independent images of the very faintest and complex astronomical targets. These goals relate directly to the limitations of existing interferometers with respect to geostationary targets, and here we explain briefly how the MROI design achieves these goals.

The MROI has been designed to be much more sensitive than existing arrays. Analyses of the global error budget for the array predict a fifty- to one-hundred-fold (50–100) improvement in sensitivity over the current best optical and infrared synthesis telescopes such as the CHARA and VLT interferometers. The faintest targets that are routinely observable with these facility class arrays today have 2.2  $\mu\text{m}$  (K band) magnitudes of between 7 and 10. This is some 3–6 magnitudes brighter than the MROI design sensitivity of  $K = 13$ . In other terms, the MROI will be able to image objects some 40 to 600 times dimmer than is possible with the current generation of ground based interferometers.

The reason for the MROI’s enhanced sensitivity is largely due to an emphasis in its design on minimizing losses: each one of its eight sequential opto-mechanical subsystems has been optimized so as to maximize optical throughput, and to minimize signal losses due to uncontrolled spatial and temporal wavefront errors. Below are a few details of the implementation adopted at the MROI which offer some pointers to the types of strategies we have adopted:

- The use of unit telescopes (UTs) designed to exhibit very low levels of internal mechanical vibration.
- The use of evacuated beam paths all the way from the UTs to the beam combination laboratory. This eliminates turbulence in the light paths from the telescopes and removes the need for any optics to compensate for longitudinal atmospheric dispersion.
- The use of light in separate wavelength channels to monitor and/or control the interferometer sub-systems so that no light from the science target need be diverted from the science instrument. For example, for a science observation at 1.25 microns, light from 0.60–1.0 microns would be used to control the low-order adaptive optics (fast tip/tilt) systems, whereas light in the 1.65 micron window would be used to monitor and control optical path length perturbations.
- The use of a single opto-mechanical system (delay line) for equalizing the optical path of the light beam from each unit telescope. Other arrays frequently use multiple delay lines to allow the optical path from each telescope to be adjusted, but in doing so multiple reflections of the light beam are necessary. The use of single-stroke delay lines at the MROI, together with other similar design features, means that the MROI optical train has roughly 10 fewer reflections from the sky to the science instrument detector than a typical implementation at a contemporary facility array with no loss of functionality.

- The use of an automated end-to-end alignment system for the full optical train, used both before target observation begins, and subsequently in a real-time mode so that as an observation is being executed the effects of any slow opto-mechanical creep are eliminated.

The second important distinguishing feature of the MROI is its emphasis on model-independent imaging of complex targets. By “model-independent” we mean that in principle nothing needs to be known beforehand about the shape of the target in order to make an image. This is to be contrasted with “parametric imaging”, used at almost all other facilities, where assumptions about the target structure have to be made before the interferometric measurements can be usefully interpreted. For example, for an astronomical observation of a star, one frequently must assume the disk is circularly symmetric before the interferometric measurements can be interpreted in terms of a stellar disk size.

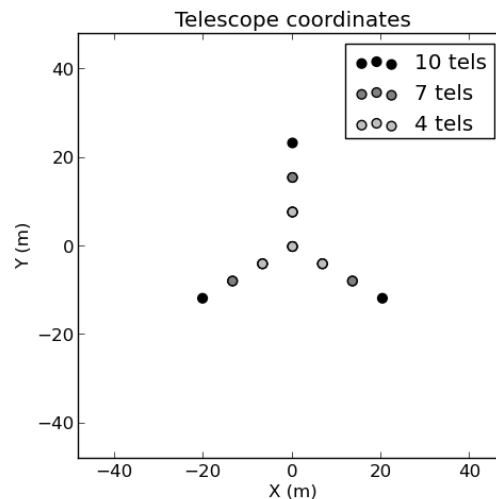


Figure 1 – Layout of the telescope arrays at the MROI. The dots represent the positions of the telescopes in the most compact array configuration. Dots of different grey shades indicate positions that would be occupied by arrays with successively larger numbers of telescopes as indicated in the legend. The inter-telescope spacing is roughly 8 m.

Several features of the MROI design contribute to this imaging goal. The most important of these have to do with the number and layout of the UTs. The telescopes are arranged in a “Y”-shaped configuration. Standard array configurations at different levels of deployment have 4, 7 or 10 telescopes present, arranged with equal nearest-neighbor distances as shown Figure 1. Because the telescopes are transportable, these array configurations can be scaled from the most compact configuration, with a minimum baseline of 7.8 m and a maximum baseline (with 10 telescopes present) of 40 m, to an extreme configuration with a maximum baseline of 346 m.

The large number of telescopes and their arrangement at the MROI gives very good instantaneous coverage of the Fourier plane ( $u$ - $v$  plane) as shown in Figure 2. This coverage allows complex objects to be imaged by allowing information on a range of spatial scales and orientations to be captured at the same time. Roughly speaking the number of independent samples available in the  $u$ - $v$  plane corresponds to the number of independent image elements (“pixels”) that can be reconstructed in the image. This number of degrees-of-freedom or “picture elements” scales roughly as the square of the number of telescopes. With 10 telescopes, the MROI will sample 3 times the number of  $u$ - $v$  points at any one time compared to its nearest rival, the 6-telescope CHARA array.

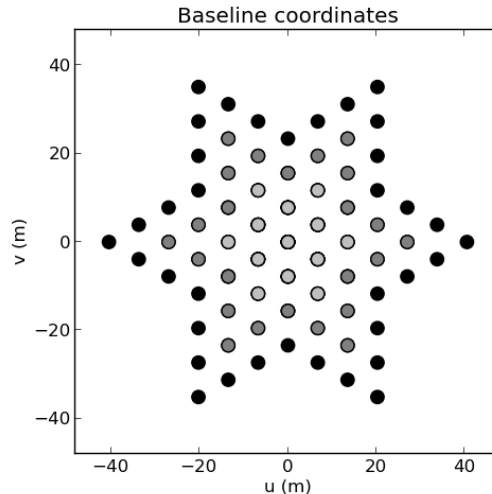


Figure 2 – Fourier plane (" $u-v$ ") coverage of the MROI for an object at the zenith. Coverage for arrays with 4, 7, and 10 telescopes is indicated by the grey levels of the dots (all arrays include the coverage of smaller arrays as subsets).

The advantage in instantaneous  $u-v$  coverage is of particular significance for GEO observations because when more conventional astronomical targets are being imaged, interferometers can make use of the rotation of the Earth with respect to the target to increase the  $u-v$  coverage of a given configuration of telescopes. This "Earth rotation synthesis" will not be possible with geostationary targets since, by definition, these remain essentially stationary in the sky relative to the observer.

The ability to "zoom" the size of the array configuration at the MROI – which for example is not possible at the CHARA interferometer – gives a corresponding zoom facility in the pixel scale of the imaging. This means that the pixel scale can be matched to that of the target for different satellite types and investigations.

Figure 3 shows the relationship between the available MROI baselines and the sizes of the features that it will be most sensitive to at various wavelengths from 0.6–2.4 microns. For example, with a 30 m interferometer baseline at 1.25 microns, a structure as small as  $\sim 1.5$  m would be "distinguishable" in a reconstructed image. As Figure 3 makes clear, the range of spatial scales that, in principle, might be probed by the MROI spans roughly two orders of magnitude, from space debris through several-meter scale buses to large 10 m long solar panels.

The ability to secure data at wavelengths from 0.6 to 2.4 microns will allow the possibility of differential interferometry/imaging of targets with structures that have albedos that vary significantly over this range of wavelengths, for example gold and typical solar panel material. These extra diagnostic capabilities affordable through multi-wavelength observations will be valuable both from a scientific and operational perspective.

For observing comparatively "large" targets such as GEO satellites, an important feature of the MROI is its separation of the roles of path length monitoring and imaging data collection to two separate beam combiners. As in all interferometers, the raw signal from any pair of telescopes in the array will be a modulated light pattern – a so-called "interference fringe" – whose properties will encode both the structure of the target and also give information about the atmosphere optical paths above the pair of telescopes being used. At the MROI two separate instruments will be used to extract these different signals simultaneously, allowing each to be optimized for its specialized task. The first instrument will be a fringe tracking beam combiner operating at a wavelength of 1.6 or 2.2 microns. This will monitor the atmospheric path length disturbances on all pairs of nearest neighbor telescopes and will thus allow the otherwise damaging effects of the atmosphere to be corrected. By tracking the fringes on the shortest nearest neighbor baselines and at the longest wavelengths, where the object is less resolved, and by taking advantage of the MROI's equispaced telescope configuration it will be possible to combine the shortest-baseline measurements to "phase up" the entire array.

The fringe tracking instrument will set the overall sensitivity of the array: if this system fails, imaging will no longer be possible and so the geometry of the MROI telescope layout is in fact critical to both setting the imaging capability and also to the sensitivity of imaging possible.

Quite separately an independent “science” beam combining instrument will operate in parallel with the fringe tracker and collect the fringe data needed for imaging on all the interferometer baselines, both long and short. This instrument can be operated at a shorter wavelength than the fringe tracker, e.g. the near-IR J band at 1.25 microns, and typically will collect data for several hundred seconds. In this way it will be possible to secure higher angular resolution data at the MROI than if the fringe tracking and science data collection functions were undertaken by the same beam combiner, since both the wavelengths and the baselines used can be optimized independently for these different roles.

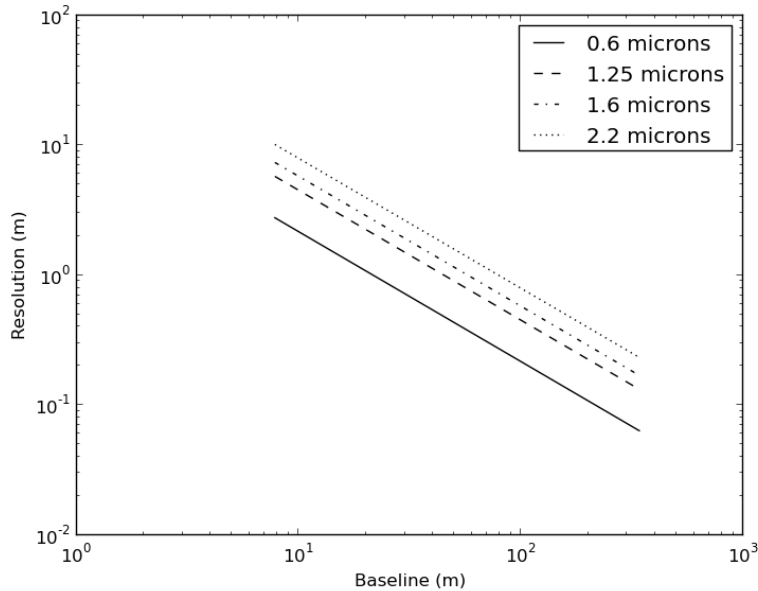


Figure 3 – The relationship between the available MROI baseline lengths, the observing wavelength and the interferometric resolution (in meters) assuming a target in a geosynchronous orbit.

All of these key design characteristics result in the MROI being a potentially powerful tool for imaging both commercial and military geosynchronous satellites. In the following two sections we examine in more detail what performance it might reasonably be expected to realize in such a role.

#### 4. SENSITIVITY MATCH TO GEO TARGETS

An important question for the imaging of any interferometric target is whether the target is bright enough, since interferometric imaging from the ground is fundamentally limited to observing relatively bright targets. Previous analyses, and observations of GEO targets (see, e.g. Bakker et al, 2009<sup>1</sup> and Hindsley et al 2011<sup>2</sup>) have suggested that useful data might only be captured during the few minutes of the year when the targets “glint” due to a favorable relative alignment between the target, the Sun and the Earth. During this period the target is very bright; however not only is the time available for imaging limited, but also the object will also appear to be dominated by the surface which is correctly aligned (usually the solar panels), and all other details will be lost in the glare from this surface.

We can estimate the apparent brightness of non-glinting targets illuminated by the sun – which will be observable for much longer periods – by assuming an average reflectance and overall target size, i.e. including solar panels. Assuming for simplicity a spherical and diffuse target with an average reflectance of 0.2, then at a wavelength of 2.2 microns (the astronomical K band) a target less than 1 m in diameter would have a K-magnitude fainter than 14, too faint to be observed with the MROI. However a target with an overall extent of 3 m would have a K magnitude of 12, well within MROI’s projected capability, and a 5 m diameter target would have a magnitude of 11, bright for MROI. All these targets would be too faint to be imaged by other arrays, with typical limiting magnitudes of 7–9.

Evidence from the literature (Payne 1998<sup>3</sup>; Payne et al 2006<sup>4</sup>) suggests that roughly 50% of GEO satellites have K band (2.2 micron) magnitudes brighter than 12.5. Some examples of photometry of GEO satellites are shown in Figure 4 (see caption for details).

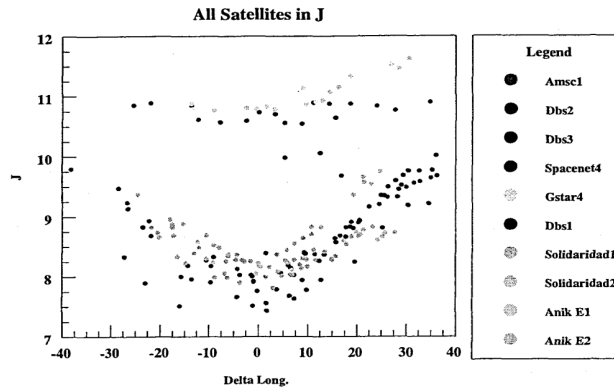


Figure 4 – Measurements of infrared magnitudes of a number of GEO satellites at 1.25 microns, from Sanchez et al, 2000<sup>5</sup>. In the H-band (1.65 microns) the objects were measured to be approximately 0.3–0.8 magnitudes brighter. The MROI, with an H-band limiting magnitude of 14, should be able to track fringes on all these targets, providing they have significant amounts of compact (< 5 m in size) structure.

These J band measurements reveal two classes of targets. The first show a characteristic brightening and then fading with increasing longitude, with excursions of as much as a factor of 10, i.e. 2.5 magnitudes. A second class show much less variation in brightness, presumably due to a smaller contribution to the total brightness from large highly infrared-reflective solar panels that are altering their orientation with respect to the observer as a function of time. Importantly, in this survey of Sanchez<sup>5</sup>, even the faintest targets had mean J band magnitudes of approximately 11. The larger datasets of Payne and colleagues<sup>3,4</sup> suggest that perhaps 50% of all GEO satellites will be visible with the MROI in the K band, assuming the typical red colors seen by Sanchez. These would imply a median K magnitude of 12.5. Payne (2010) also confirms that a magnitude sensitivity of 12 in the astronomical R-band would catch 50% of all targets<sup>6</sup>.

While the MROI will certainly be able to detect targets with a K magnitude of 12.5, a more important question is whether it will be able to routinely provide reliable images of such targets. The ability of a ground-based interferometer to image a target depends crucially on how resolved the target is on the baselines that are being measured. For a “good” image to be recovered, the interferometer must secure data on long enough baselines that the smallest structures are appropriately resolved, but also on much shorter baselines so that the larger scale features of the target are detected and recovered too. The range of physical scales of interest in the target – which might for example run from a less than a meter (i.e. less than the diameter of a typical main antenna) to 15 meters (the length of a large solar panel) – will thus act as important drivers for the amount and quality of data that must be secured.

At many long baseline interferometers, for example the CHARA array at Mt. Wilson and the Navy Optical Interferometer in Flagstaff, this need to secure data on a wide range of interferometer baselines has been problematic. This has arisen primarily for three reasons:

- There may be too few unit telescopes to permit a wide range of inter-telescope separations to be realized without necessitating physical movement of the telescopes.
- Even if there are a suitable number of telescopes, it may not always be possible to combine beams from all in an efficient way.
- The signal-to-noise (S/N) ratio for measurements made with an optical/infrared interferometer is a strong function of how well resolved the target is. On baselines where the target is well resolved the S/N will be low, and so it may be difficult to secure reliable and hence useful data.

At the MROI, the design of the array infrastructure has been optimized specifically to allow these difficulties to be overcome. Notably:

1. The MROI will utilize up to 10 telescopes simultaneously, although its initial deployment will be with fewer telescopes.
2. The MROI will utilize a multi-way science beam combiner so that as many inter-telescopes baselines can be interrogated at once as is reasonably possible.

3. The MROI will incorporate a fringe tracker (a separate instrument from the science instrument), which will monitor the atmospheric disturbances on the shortest nearest-neighbor baselines and stabilize the array against the atmosphere. This has been designed to operate at very low flux levels, corresponding to  $K = 13$ , i.e. 0.5 magnitudes fainter than the median flux levels expected for a wide range of GEO targets of interest.

A preliminary assessment of the range of common GEO bus and payload sizes suggests that it is likely that a reasonable fraction of targets will be compact enough to give high signal-to-noise interference fringes on the short fringe tracker baselines. Under these conditions, active control of the atmospheric fluctuations should be straightforward, and hence the science measurements needed to allow the reconstruction of a high-resolution image will be feasible. The reader should note that with an interferometer, if measurements are made of two targets of the same apparent brightness but of different size, the more compact target will in general provide data of much higher signal-to-noise. For the MROI, we use the term “compact” here to identify sources at GEO where 50% or more of the total light from the target comes from a region no more than about 5 m across. This is comparable to the brightest components of a typical bus and payload when seen in projection, and this definition, importantly, does not preclude targets that have much larger solar panels attached unless these are oriented such that the return from the target is dominated by a high-intensity glint off these.

Notwithstanding the discussion of the previous paragraph, modern image reconstruction codes can make good use of interferometric data even when some of the structure is “washed out” due to over-resolution by the interferometer baselines – see, for example, the simulations below. In addition, even fainter targets might be accessible if they were observable in the H band (where the fringe tracker sensitivity is somewhat better), provided they were dominated by more compact flux.

In summary, we expect that overall a significant proportion of the GEO population is likely to be accessible to the MROI. These targets would be observable even when the solar panels are not glinting – allowing the whole target to be inspected without being blinded by the “glare” of a glint. Furthermore multi-color data would allow characterization of the targets and follow-up imaging with scaled array configurations could conceivably probe scales as small as tens of centimeters.

## 5. IMAGING PERFORMANCE

Having determined that there are likely to be a sufficient number of targets that will be bright enough to be imaged with the MROI, a second key question concerns the kind of images one might reasonably expect to obtain. As with all interferometric synthesis arrays, the process of imaging is a post-observing procedure which takes as input a large number of the measurements of the interference fringes generated by the pairs of telescopes in the array, and recorded by the science beam combiner instrument. Each of these recorded fringes encodes the amplitude and phase of a particular Fourier component of the target brightness distribution. An image is then reconstructed by an iterative procedure which determines the most probable image consistent with the data. These reconstruction techniques have been developed, understood, and used routinely and successfully for imaging at radio, millimeter and optical/infrared wavelengths for many years now, albeit not optimized for GEO targets.

Several heuristic arguments, developed and verified through many years of interferometric imaging at radio wavelengths, constrain the type of imaging that can be realized with any interferometer. The first is that  $R$ , the ratio of shortest to longest baseline, sets the range of angular scales measured.  $R$  is governed by the number of telescopes in an array and takes values of 1.7, 3.5, and 5.2 for the 4-, 7- and 10-telescope implementations of the MROI. A-priori information, e.g. positivity of the target flux, is needed to constrain structures on other angular scales. The second “rule of thumb” is that the total number of degrees of freedom in any recovered image should not significantly exceed the number of independent visibility data measured. The term “number of degrees of freedom” basically quantifies how complicated a target image might be: roughly speaking, if an image can be decomposed into say  $N$  independent and individually simple elements then we can say it has  $N$  degrees of freedom. For an interferometer with 10 telescopes up to 45 different baselines, i.e. 45 sets of fringe data, can be measured, so the number of “degrees of freedom” in any recovered image, i.e. the number of independent resolution elements, is expected to be of the order of 50 or so.

We can thus estimate that with the full 10-telescope complement of the MROI it will be routinely possible to make images containing approximately 50 independent resolution elements. Depending on the precise array layout being used, these could distinguish, for example, 70 cm features on a 5-meter bus and payload, or 30 cm features on a satellite or piece of space debris a factor of roughly two times smaller. Earlier phases of deployment of the MROI with smaller

numbers of telescopes could have a similar angular resolution but would be less able to separate out complicated image structures.

In both cases, simultaneous imaging in multiple spectral channels to give a “hyperspectral” image cube would be available. This would typically provide 5–70 channels across the 1.2–1.3 micron, 1.5–1.8 micron, or 1.9–2.4 micron wavebands. For a subset of targets it might also be possible to extract key diagnostics on features as small as 10 cm, depending on the image structure and brightness.

### 5.1 Imaging simulation

We have performed simulations of MROI imaging for two representative GEO targets, in order to assess the likely impact of the spatial-frequency sampling and realistic fringe data signal-to-noise. Simulated datasets were prepared by evaluating the discrete Fourier transform of suitably scaled model images at spatial frequencies corresponding to the assumed MROI interferometric projected baselines. Model images were simulated using the TASAT software<sup>7</sup>. The targets were assumed to have a constant structure across the spectral channels of the science beam combiner. The Fourier data were then used to generate “perfect” values of the relevant interferometric observables, i.e. squared visibilities and bispectra. Random errors were added to these values so as to properly mimic the signal-to-noise that would have been expected given various target magnitudes, the predicted interferometric performance, e.g. coherence losses due to jitter etc., and the assumed detector performance. In addition, calibration errors on the visibilities and closure phases were added. These were presumed uncorrelated and were at the level of  $\Delta V^2/V^2 = 0.02$  and 0.8 degrees for the closure phases. We assumed the presence of a switchable science beam combiner which mixes 6 beams together simultaneously (using 192 pixels per spectral channel to sample the spatially-encoded fringes), and  $4e^-$  readout noise

The simulated squared visibilities and bispectra were saved in the OIFITS format<sup>8</sup> and used as input to the BSMEM image reconstruction code<sup>9</sup>. For each dataset, a two-step reconstruction procedure was employed, similar to that used for previous BSMEM entries to the IAU-sponsored beauty contests<sup>10</sup>. First, higher-spatial frequency data were removed and BSMEM run with a uniform disk prior image. High spatial frequencies and noise were removed from the BSMEM output image by convolving with a circular Gaussian and setting pixel values below a user-selected threshold to zero. The resulting image was used as a prior for a second run of BSMEM on the full dataset.

Figure 5 shows results of imaging simulations for a range of assumed target brightnesses and sizes relative to the angular resolution of the interferometer array. The satellite used for these simulations comprises a pair of large solar panels and a more compact central bus, this type of structure being a common one for GEO satellites. In all cases the most compact 10-telescope MROI configuration was assumed, with science data being secured in the astronomical K-band (2.0–2.4 micron). The K-band magnitudes used were 8 (somewhat optimistic for a GEO target, used to show the limiting effects of the Fourier-plane coverage for moderate signal-to-noise data) and 11 (a more realistic brightness). The MROI fringe tracking combiner is predicted to have sufficient signal-to-noise to track on the latter target effectively on the nearest-neighbour baselines, despite needing to operate at a shorter wavelength where the target is more resolved. The mean signal-to-noise of the squared visibilities measured by the science combiner in 100 seconds ranged from 4.8 (for the larger K=11 target) to 12.5 (for the smaller K=8 target). The mean closure phase error ranged from 1.5 degrees to 54 degrees. In the latter case there is a noticeable impact on the quality of the imaging (see middle left panel of Figure 5).

The major features of the satellite have been reconstructed successfully, including the shape and orientation of the solar panels and the main features of the satellite bus. Reconstructing meter-scale or smaller structures on the bus is inherently problematic for targets with a pair of solar panels spanning 20–30 m, as this range of scales exceeds that which a single interferometer configuration is sensitive to (set by the ratio of the longest to the shortest baseline). State-of-the art image reconstruction algorithms provide a degree of super-resolution (typically a factor 2 for moderate S/N) which mitigates but does not remove this difficulty. The issue could be addressed by combining MROI data with low-spatial frequency data from a filled-aperture telescope, by incorporating an *a priori* model for the solar panels (fitting for the unknown orientation), or, for smaller satellites, by using two different MROI configurations.

For targets where the panels are comparable in size to the bus, imaging the details of the bus is more straightforward, as illustrated by the results in Figure 6. Here the satellite size was adjusted to match the resolution of the telescope array, and as a result the shapes of the bus and solar panel and the smaller-scale brightness variations across the bus have been accurately reconstructed. A greater degree of super-resolution is evident in the K=8 reconstruction owing to the higher signal-to-noise (by a factor of  $\sim 3$  for the squared visibility data and  $\sim 20$  for the closure phases) of the input Fourier data.



Further algorithm development to tune existing interferometric image reconstruction codes to better match the structural elements characteristic of geosynchronous targets (e.g. by using a more appropriate regularization than the maximum entropy approach used by BS MEM) is also likely to give superior imaging capabilities.

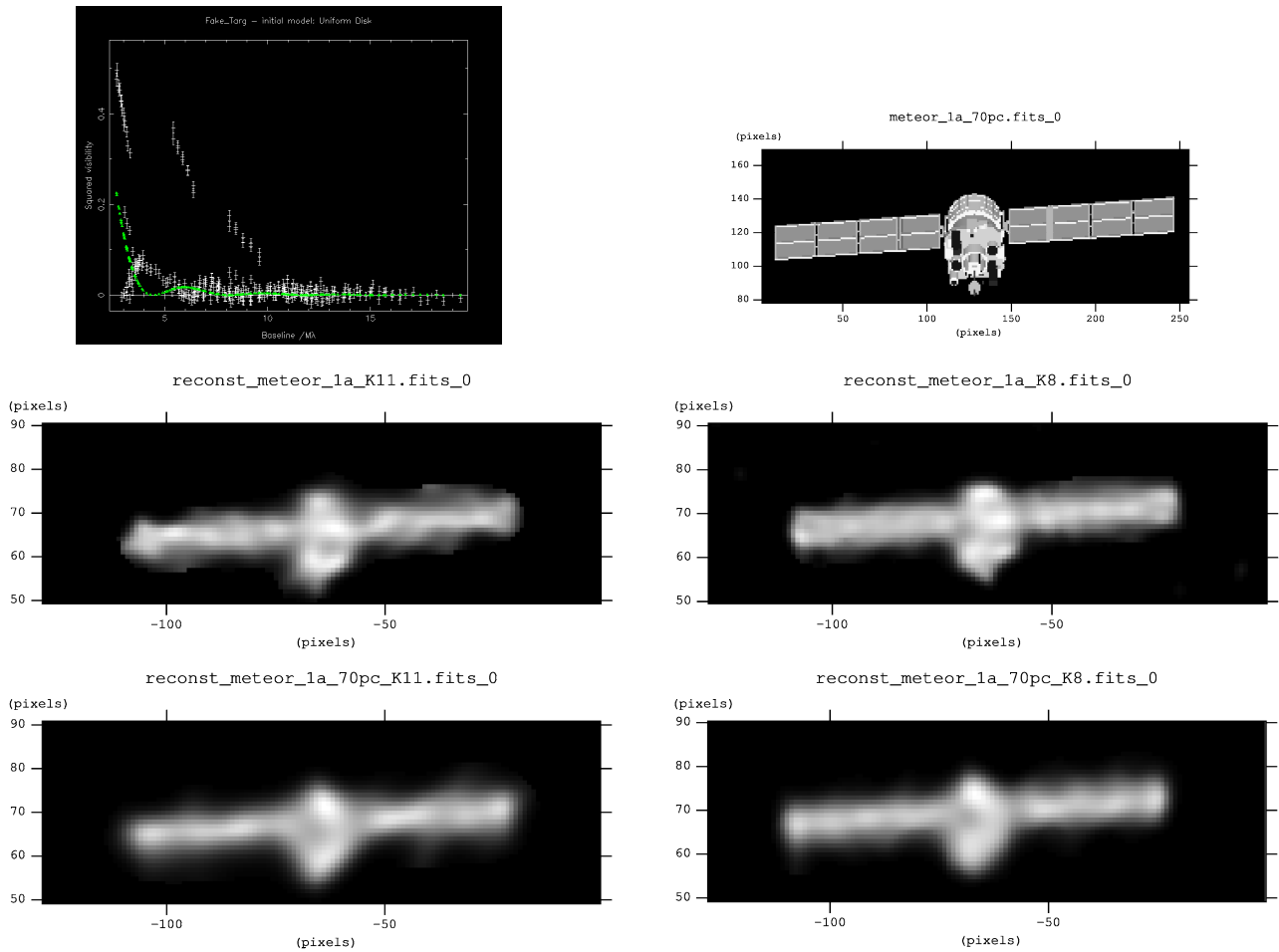


Figure 5 – Truth (top row) and reconstructed (middle and bottom rows) images for a simulated MROI observation of a typical satellite with a pair of large solar panels. A plot of the simulated squared visibilities against projected baseline length is shown at top left (a 10 m uniform disk is also plotted for comparison). Each simulated observation consisted of  $5 \times 100$  second integrations using 6-telescope sub-arrays of the most compact 10-telescope MROI configuration, and used 5 spectral channels between 2.0 and 2.4 microns (i.e. the astronomical K band). Satellite brightnesses of 11<sup>th</sup> magnitude (left column and visibility plot) and 8<sup>th</sup> magnitude (right column) in the K band were assumed. The simulation and image reconstruction parameters are detailed in the text. The maximum extent of the target, spanning the long solar panels, was 23.7 m (middle row) and 16.6 m (bottom row) respectively. These sizes correspond to the typical size of large communications satellites, and to 70% of this size which is a better match to the spatial frequencies sampled by the most compact MROI array at K band. The shape of the large solar panels is reconstructed more accurately for the compact target, reflecting the better sampling of lower spatial frequencies. The reconstruction of the K=11 larger satellite (middle left) is significantly noisier than the other three, owing to poor signal-to-noise on the long-baseline closure phase data.

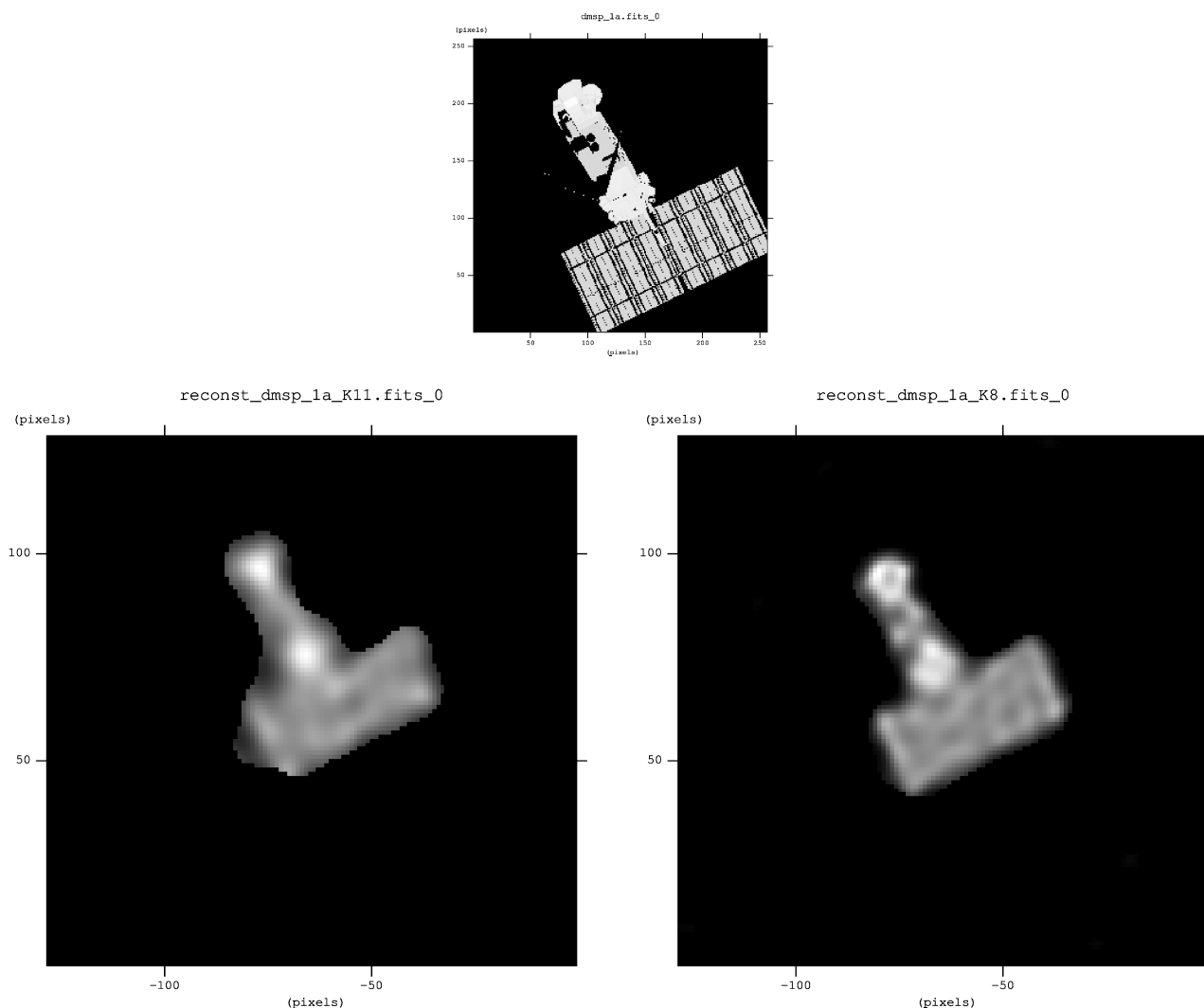


Figure 6 – Truth (top row) and reconstructed (bottom row) images for a simulated MROI observation of a satellite with a bus and solar panel of comparable size. Satellite brightnesses of 11<sup>th</sup> magnitude (left image) and 8<sup>th</sup> magnitude (right image) in the K band were assumed. The remaining simulation parameters were identical to those for Figure 5. The long dimension of the solar panel was set to be 11.9 m, approximately equal to the fringe spacing on the shortest baseline.

## 6. CONCLUSIONS

We have outlined the key design features of the MROI and have concluded that it offers an unprecedented new capability in GEO imaging. Preliminary simulations of satellite imaging with MROI are showing an impressive level of fidelity even without optimization of the algorithms for GEO targets. The MROI capitalizes on both significantly enhanced sensitivity compared with existing ground based interferometer arrays and also on significantly higher ( $> 10\times$ ) resolution as compared to any ground-based AO-corrected telescope likely to be deployed in the next 10–20 years.

## ACKNOWLEDGMENTS

The Magdalena Ridge Observatory (MRO) interferometer is hosted by the New Mexico Institute of Mining and Technology (NMIMT) in Socorro, NM, USA, in collaboration with the University of Cambridge, UK. MRO is funded by Agreement No.N00173-01-2-C902 with the Naval Research Laboratory and an institutional revenue bond issued by NMIMT. We wish to also acknowledge funding for Cambridge University staff from STFC in the UK.

## REFERENCES

- [1] Bakker, E. J., Cormier, C., Romero, V. "Imaging of geostationary satellites with the MRO interferometer," Proc. Advanced Maui Optical and Space Surveillance Technologies Conference, E58 (2009)
- [2] Hindsley, R. B., Armstrong, J. T., Schmitt, H. R., Andrews, J. R., Restaino, S. R., Wilcox, C. C., Vrba, F. J., Benson, J. A., Di Vittorio, M. E., Hutter, D. J., Shankland, P. D. and Gregory, S. A. "Navy Prototype Optical Interferometer observations of geosynchronous satellites," Applied Optics, 50, 2692 (2011)
- [3] Payne, T. E. "Target selection database," Schafer Corporation (1998)
- [4] Payne, T. E., Gregory, S. A., Kim, L. "Electro-optical signatures comparisons of geosynchronous satellites," Proc. 2006 IEEE Aerospace Conference, 1 (2006)
- [5] Sanchez, D. J., Gregory, S. A., Werling, D., Payne, T. E., Kann, L., Finkner, L. G., Payne, D. M., Davis, C. K. "Photometric measurements of deep-space satellites," Proc. SPIE 4091, 164 (2000)
- [6] Payne, T. E, priv. comm. (2010)
- [7] Riker, J. F. and Butts, R. R. "The time-domain analysis simulation for advanced tracking (TASAT) approaches to compensated imaging," Proc. SPIE 1688, 548 (1992)
- [8] Pauls, T. A., Young, J. S., Cotton, W. D. and Monnier, J. D. "A data exchange standard for optical (visible/IR) interferometry," PASP 117, 1255 (2005)
- [9] Baron, F. and Young, J. S. "Image reconstruction at Cambridge University," Proc. SPIE 7013, 70133X (2008)
- [10] Malbet, F. et al "The 2010 interferometric imaging beauty contest," Proc. SPIE 7734, 77342N (2010)